The Rollover Risk and its Mitigation in Rickshaws

Edgar A. Vázquez-Rodríguez, Francisco J. Perez-Pinal, and Pedro Bautista-Camino
Electronics Department
Instituto Tecnológico de Celaya
Antonio García Cubas 600, Col. FOVISSSTE, Celaya, Guanajuato, México
M1703086@itcelaya.edu.mx,
francisco.perez@itcelaya.edu.mx,
d1803004@itcelaya.edu.mx

Martín A. Rodríguez-Licea
Electronics Department
CONACYT-Instituto Tecnológico de Celaya
Antonio García Cubas 600, Col. FOVISSSTE, Celaya, Guanajuato, México
martin.rodriguez@itcelaya.edu.mx

***Abstract*—Although there are important efforts to electrify and diversify small vehicles, active safety on motorcycles and tricycles (also known as autorickshaw, tuk-tuk, mototaxi, etc.) has been relegated. For example, the electric tricycles marketed (and even internal combustion ones), don't integrate an active safety system that prevents or mitigates the risk of rollover, despite how prone they are to such a situation; the concern for the increase in its commercialization is latent and unfortunately, there are very few scientific studies related. In this article, the obtaining and validation of a new rollover index for tricycles is presented and it is shown the effectiveness to predict and detect the risk even statically. In addition, a controller for the mitigation of the rollover risk and a Laplace-based stability analysis are presented, where the controller consists in performing a differential braking with the rear wheels; the effectiveness of the proposed strategy is illustrated with CarSim simulations.**

I. Introduction

Nowadays, there exists a concern due to the rise in vehicle traffic and to the high levels of pollution in cities. An alternative to prevent such problems is the use of smaller vehicles, mostly because of their lightweight, narrow design, and fuel-efficient. Three-wheeled vehicles are used as a form of public transport in different countries like India, Thailand, China and even Italy [1]–[3] and are regularly named tuk-tuks, bicitaxis, rickshaws, among others. Moreover, electric vehicles are considered a potential competitor for three and four-wheeled vehicles [4], [5]. Electric vehicles have the major advantage of lower fuel consumption and even zero emissions to the environment. In recent years the introduction of electric four-wheel vehicles has had a good acceptance with significant statistics in the global market because of the high cost and limited availability of fossil fuels [6], [7]. Additionally, it seems natural to introduce the use of three-wheeled vehicles as a form of personal transportation due to their narrow design, lightweight, energy efficiency, and easy driving and parking. The main disadvantage that difficult the possibility of better acceptance of this kind of vehicles, is their low stability in curves, compared with conventional four-wheel vehicles. This is to say, to be an acceptable alternative for transportation, these vehicles should be as comfort and safety as an average passenger car.

Since the end of the last century, a rapid development has been established in terms of safety in vehicles. The National Highway Traffic Safety Administration (NHTSA) [8], a dependency of the Transport Department of the U.S. government, has motivated the improving of active and passive safety in vehicles. As a result, important investigations have been performed resulting in the publication of new safety standards and scientific literature about active safety in four-wheeled vehicles, many of them developing rollover prevention/mitigation techniques (see [9]–[17] *et al.*) The North American Free Trade Agreement (NAFTA) define the Load Transfer Ratio (LTR) as the relative roll instability associated with the loss of tire contact with the road. The LTR is also known in the literature as Lateral Load Transfer (LLT) [18], [19] and Rollover Index (RI) [20]–[22], and is defined as a measurement of rollover risk by detecting if a wheel is about to lose ground contact. The rollover risk estimation is not enough to mitigate an accident risk, therefore, an active control is necessary; however, while contributions for four-wheel vehicles are varied, the landscape for tricycles in terms of contributions is scarce. In [23], the author present a preventing device of rollover for three-wheeled vehicles; the controller activates different actuators that are used to prevent or reduce the rollover conditions, but the control methodology seems to be static so it is not proven that the device dynamically mitigates the rollover. A reactive rollover system for three-wheeled vehicles with Delta or Tadpole configuration is established by the author of [24]; despite the use of independent brakes as an actuator, the system does not consider the vehicle dynamics such that the rollover is mitigated only in specific conditions. In [25], the author performs an analysis of a three-wheeled vehicle model with Tadpole configuration; model simulations are performed with Adams Multibody Dynamics and with MATLAB to evaluate the behavior of the suspension for diverse maneuvers and scenarios. The authors do not propose a control methodology to manipulate the model variables. In [26], the authors use the Adams Car software to obtain a numerical model of a three-wheeled vehicle in order to study the instability (wooble) by comparing the dynamics of a multibody model and a rigid body model; this work aims to perfect the dynamics of a

978-1-5386-5935-9/18/$31.00 ©2018 IEEE

tricycle in an early design stage. The authors in [27] and [28] study the dynamics of tricycles using 4 and 6 degrees of freedom (DOF) models, respectively. The application of a control system is left as a future job.

In this article, a dynamic model and rollover index for a three-wheel vehicle with a Delta configuration (a single tire in the front and two rear tires) is presented. The mathematical model is validated (in a closed loop scenario) with CarSim (a mechanical simulation software used extensively for wheeled vehicle designs) and Simulink environments. The RI analogously as four-wheeled vehicles gives a perception of the unbalance between the rear vertical forces in the rear tires through a percentual value with sign. The sign means to which side the risk is present and the magnitude shows how close it is to rollover (e.g. 1 means an imminent rollover to the left). Later, a rollover mitigation/prevention controller is designed using rear differential braking as an actuator and a Laplace-based stability analysis is presented. Finally, illustrative simulations in closed loop with CarSim are presented. This paper is organized as follows: the mathematical model of the tricycle is presented in Section II, a rollover index estimation for a three-wheeled vehicle is presented in Section III. The proposed controller is detailed in Section IV followed by the illustrative simulations in Section V. Lastly, conclusions are presented in section VI.

II. The Tricycle Model

A. Tire Side Slip Angle

In Figure 1 are shown relevant variables of the dynamic behaviour of the tricycle. In this paper it is considered that the origin of $\sum In$ is at a considerable distance from the center of gravity (CoG) such that the rear wheels can be seen as a single one and the vertical movement components of the CoG are negligible [29]. By the consideration above $v_{wf} \approx v_{CoG}$, and considering $v_{wf} > 0$, hence the lateral front wheel speed is obtained:

$$v_{wf}\sin(\delta - \alpha_f) = l_F\dot{\psi} + v_{CoG}\sin(\beta) \tag{1}$$

and in the longitudinal direction:

$$v_{wf}\cos(\delta - \alpha_f) = v_{CoG}\sin(\beta) \tag{2}$$

where w_{wf} is the front wheel speed, δ is the front wheel steering angle, α_f is the front tire sideslip angle, l_f is the distance from the center of the front axle wheel to the CoG, ψ is the angle around of the vertical axis, v_{CoG} is the magnitude of the speed of the CoG, and β is the sideslip angle from the CoG. The terms in the left side of the Equation (1), represent the wheel speed, while the terms in the right side represent the chassis speed about the CoG. Dividing Equation (1) by (2) and due to the small δ angle (in normal operation conditions), α_f and β are assumed as small angles, then $\sin(\beta) \approx \beta$, $\cos(\beta) \approx 1$, and $\tan(\alpha_f) \approx \alpha_f$:

$$\alpha_f = \delta - \beta - \frac{l_f\ \dot{\psi}}{v_{CoG}} \tag{3}$$

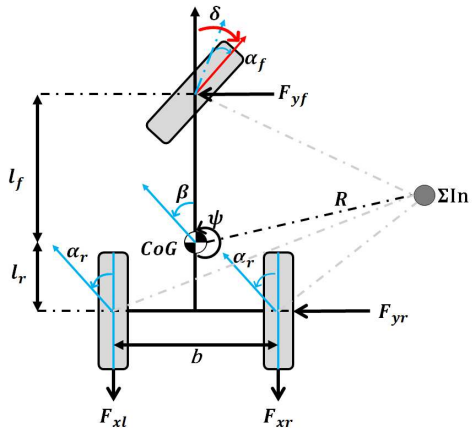

Fig. 1. Tricycle model aproximation.

$$\alpha_r = \frac{l_r\ \dot{\psi}}{v_{CoG}} - \beta \tag{4}$$

where α_r is the rear wheel side slip angle and l_r is the distance from the center of the rear axle wheel to the CoG.

B. Rotational Dynamics

The forces acting around the CoG of the tricycle vehicle are [30], [31]:

$$\begin{bmatrix}\ddot{x}_{CoG}\\ \ddot{y}_{CoG}\end{bmatrix} = \frac{1}{m_{CoG}}\begin{bmatrix}\sum F_x\\ \sum F_y\end{bmatrix} \tag{5}$$

where m_{CoG} is the mass of CoG, F_x and F_y are the longitudinal and lateral forces in the contact points of the wheels with the ground in its components X and Y respectively; the lateral forces interacting in the front and rear wheels are:

$$\sum F_y = F_{yf} + F_{yr} \tag{6}$$

where, F_{yf} are the sum of the lateral forces acting in the rear axle while F_{yr} is the lateral force in the front wheel. The front lateral force can be approximated in normal operating conditions by [29]:

$$F_{yf} = C_{\alpha f}\alpha_f \tag{7}$$

and for the rear wheels:

$$F_{yr} = C_{\alpha r}\alpha_r \tag{8}$$

where $C_{\alpha f}$ is the cornering stiffness on the front tire and $C_{\alpha r}$ is the cornering stiffness on the rear tires. Substituting (7) and (8) in (6):

$$\sum F_y = C_{\alpha f}\alpha_f + C_{\alpha r}\alpha_r \tag{9}$$

On the other hand, performing a torque balance around the vertical axle (Figure 1):

$$J\ddot{\psi} = l_f F_{yf} - l_r F_{yr} + b_l F_{xrl} - b_r F_{xrr} \tag{10}$$

where J is the yaw moment of inertia, b_l is the distance from the left rear wheel center to the chassis longitudinal axis, b_r is the distance from the right rear wheel center to the chassis

longitudinal axis, F_{xrl} and F_{xrr} are the braking forces from the left and right wheels. By substituting F_{yf} and F_{yr} from (7) and (8):

$$J\ddot{\psi} = l_f C_{\alpha f}\alpha_f - l_r C_{\alpha r}\alpha_r + b_l F_{xrl} - b_r F_{xrr} \tag{11}$$

Substituting α_f and α_r from (3) and (4):

$$\begin{aligned}\ddot{\psi} &= \left[\frac{l_f C_{\alpha f}}{J}\right]\delta + \left[\frac{l_r C_{\alpha r} - l_f C_{\alpha f}}{J}\right]\beta \\ &- \left[\frac{l_f^2 C_{\alpha f} + l_r^2 C_{\alpha r}}{J v_{CoG}}\right]\dot{\psi} + \left[\frac{b_l F_{xrl}}{J} - \frac{b_r F_{xrr}}{J}\right]\end{aligned} \tag{12}$$

The above equation describes the dynamic behavior of the yaw acceleration.

C. Translational Dynamics

From the inertial coordinate system and the Newton laws:

$$m_{CoG}\begin{bmatrix}\ddot{x}_{In}\\ \ddot{y}_{In}\\ \ddot{z}_{In}\end{bmatrix} = T_{UI}\left[F_{yf} + F_{yr} + F_{xrl} + F_{xrr}\right] \tag{13}$$

where T_{UI} is a transformation matrix used to rotate from the chassis to the inertial coordinate system. Again, the vertical acceleration from the CoG is neglected, and the trigonometric decomposition of v_{CoG}, is obtained:

$$\begin{bmatrix}\dot{x}_{In}\\ \dot{y}_{In}\end{bmatrix} = v_{CoG}\begin{bmatrix}\cos(\beta+\psi)\\ \sin(\beta+\psi)\end{bmatrix} \tag{14}$$

By differentiation and transformation from inertial coordinate system to the chassis coordinate system:

$$\begin{bmatrix}\ddot{x}_{CoG}\\ \ddot{y}_{CoG}\end{bmatrix} = v_{CoG}(\dot{\beta}+\dot{\psi})\begin{bmatrix}-\sin\beta\\ \cos\beta\end{bmatrix} + \dot{v}_{CoG}\begin{bmatrix}\cos\beta\\ \sin\beta\end{bmatrix} \tag{15}$$

By substituting (5) in (15) and solving for $\dot{\beta}$, it turns on [30]:

$$\dot{\beta} = \frac{F_{yf} + F_{yr}}{m_{CoG} v_{CoG}} - \dot{\psi} \tag{16}$$

Substituting F_{yf} and F_{yr} from (7), (8), (3) and (4):

$$\begin{aligned}\dot{\beta} &= \left[\frac{C_{\alpha f}}{m_{CoG} v_{CoG}}\right]\delta - \left[\frac{C_{\alpha f}+C_{\alpha r}}{m_{CoG} v_{CoG}}\right]\beta \\ &+ \left[\frac{l_r C_{\alpha r} - l_f C_{\alpha f}}{m_{CoG} v_{CoG}^2} - 1\right]\dot{\psi}\end{aligned} \tag{17}$$

where δ is considered an exogenous perturbation, β and $\dot{\psi}$ are the system's states and F_{xrl}, F_{xrr} are the control inputs representing the braking force in the left and right rear wheels respectively.

III. Rollover Index

It is well known, that a rollover condition is obtained from a wheel vertical forces unbalance [19], [18]. The LTR is defined as the normalized difference between the vertical forces on the left and right wheel-ground contact points [32]:

$$LTR = \frac{\sum F_{ZR} - \sum F_{ZL}}{\sum F_{ZR} + \sum F_{ZL}} \tag{18}$$

where F_{ZR} is the sum of the right vertical forces on the wheel-ground contact point and respectively F_{ZL} for the left forces sum. In this article, it is not considered the case when the front wheel or both rear wheels lose contact from the ground. Assuming such consideration, the vertical forces acting in (18) are only F_{zrl} and F_{zrr}. Analogously to four-wheeled vehicles, it is proposed that the new rollover index for tricycles to be the normalized difference of the vertical forces at the wheel-ground contact points of the rear wheels:

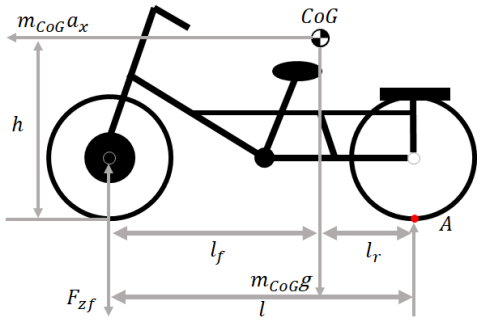

Fig. 2. Vertical forces at the contact points (side view).

$$RI = \frac{F_{zrl} - F_{zrr}}{F_{zrl} + F_{zrr}} \tag{19}$$

where F_{zrl} represents the vertical force in the wheel-ground contact point of the left rear wheel and analougsly F_{zrr} stands for the right rear wheel. From the above equation, if $RI = 1$ then $F_{zrr} = 0$ and a rollover to the left is imminent; $RI = 0$ means that $F_{zrl} = F_{zrr} = 0$ showing no risk of rollover; $RI = -1$ goes for $F_{zrl} = 0$ and a rollover to the right is imminent.

A. Rollover Risk Estimation

From the Figure 2, a torque balance with respect to the point A and from the front to the rear is:

$$F_{zf} = \frac{l_r m_{CoG} g}{l} + \frac{h m_{CoG} a_x}{l} \tag{20}$$

where F_{zf} is the vertical force at the front wheel in the wheel-ground contact point, l is the distance from the front wheel axle to the rear wheel axle, g is the gravitational acceleration ($9.81 m/s^2$), h is the height of the CoG, and a_x is the longitudinal acceleration of the CoG. Considering v_{CoG} as a constant, it gives $a_x \approx 0$ and is obtained:

$$F_{zf} = \frac{l_r m_{CoG} g}{l} \tag{21}$$

Using the Figure 3 and performing a torque balance with respect to the point B and from right to left:

$$-bF_{zrr} - \frac{b}{2}F_{zf} + b_l m_{CoG} g + h m_{CoG} a_y = 0 \tag{22}$$

where b is the width from the rear left wheel axle to the rear right wheel axle, b_r is the distance from the rear right wheel to the CoG, b_l is the distance from the rear left wheel to the CoG, a_y is the lateral acceleration of the CoG. On the other

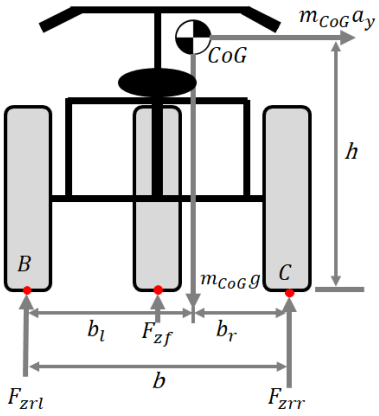

Fig. 3. Vertical forces at the contact points (rear view).

hand, performing a right-to-left torque balance with respect to the point C:

$$bF_{zrl} + \frac{b}{2}F_{zf} - b_r m_{CoG} g + h m_{CoG} a_y = 0 \tag{23}$$

Using Equation (21) and substituting in (22) and (23), is obtained:

$$F_{zrr} = \frac{b_l m_{CoG} g}{b} + \frac{m_{CoG} h a_y}{b} - \frac{l_r m_{CoG} g}{2l} \tag{24}$$

$$F_{zrl} = \frac{b_r m_{CoG} g}{b} - \frac{m_{CoG} h a_y}{b} - \frac{l_r m_{CoG} g}{2l} \tag{25}$$

Equations (24) and (25) are substituted on (19):

$$RI = \frac{l(b_r - b_l)}{b l_f} - \frac{2hla_y}{bgl_f} \tag{26}$$

The obtained RI gives a perception of the variables that contribute to lift a wheel from the ground. It is worth to mention that, generally, the location of the CoG is not laterally centered ($b_r \neq b_l$) and such that this situation constitutes a permanent contribution to the rollover risk. In addition, values of $a_y > 0$ with the CoG closer to the front wheel ($l_f \approx 0$) also represent a constant contribution to the RI.

B. Lateral Acceleration Estimation

Since the Equation (26) depends on a_y, the Newton's second law is used to estimate a model that describes the lateral acceleration depending on the state variables β and $\dot{\psi}$ and the δ input:

$$a_y \approx \frac{F_{yf} + F_{yr}}{m} \tag{27}$$

Using (7), (8), (3) and (4), it is obtained:

$$a_y \approx \left[\frac{C_{\alpha f}}{m_{CoG}}\right]\delta - \left[\frac{C_{\alpha f} + C_{\alpha r}}{m_{CoG}}\right]\beta + \left[\frac{l_r C_{\alpha r} - l_f C_{\alpha f}}{m_{CoG} v_{CoG}}\right]\dot{\psi} \tag{28}$$

Finally, by replacing the lateral acceleration in Equation (26):

$$\begin{aligned} RI &= \frac{l(b_r - b_l)}{b l_f} - \frac{2hl}{bgl_f}\left(\frac{C_{\alpha f}}{m_{CoG}}\delta\right. \\ &- \left.\frac{C_{\alpha f} + C_{\alpha r}}{m_{CoG}}\beta + \frac{l_r C_{\alpha r} - l_f C_{\alpha f}}{m_{CoG} v_{CoG}}\dot{\psi}\right) \end{aligned} \tag{29}$$

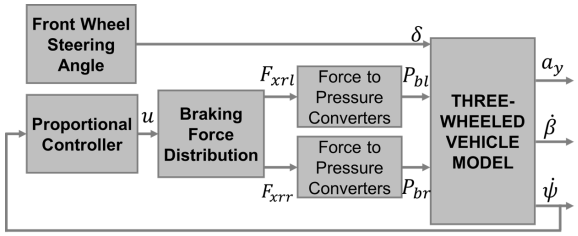

Fig. 4. Block diagram of the proposed controller.

It is worth to mention that a CarSim validation was performed showing very accurate model dynamics and rollover risk estimations during normal driving conditions (before the rollover occurs); obviously the model is not useful for situations when a wheel has lost wheel-ground contact, this is, for post-rollover dynamic. Such validation is not presented here because of the paper length limitation.

IV. Controller Design

In this paper, it is considered that the CoG is laterally centered ($b_l = b_r$); it will be left as a future work the case $b_l \neq b_r$. With the previous assumption, the RI is reduced to a state and front wheel steering angle dependence; the space state model of the dynamic system can be written as:

$$\dot{x} = Ax + Bu + C\delta \tag{30}$$

where

$$A = \begin{bmatrix} -\frac{C_{\alpha f}+C_{\alpha r}}{m_{CoG}v_{CoG}} & \frac{C_{\alpha r}l_r + C_{\alpha f}l_f}{m_{CoG}v_{CoG}^2} - 1 \\ \frac{C_{\alpha r}l_r - C_{\alpha f}l_f}{J} & -\frac{C_{\alpha r}l_r^2 + C_{\alpha f}l_f^2}{Jv_{CoG}} \end{bmatrix}, B = \begin{bmatrix} 0 & 0 \\ \frac{b_l}{J} & \frac{b_r}{J} \end{bmatrix},$$

$$C = \begin{bmatrix} \frac{C_{\alpha f}}{m_{CoG}v_{CoG}} \\ \frac{C_f l_f}{J} \end{bmatrix}, x = \begin{bmatrix} \beta \\ \dot{\psi} \end{bmatrix}, u = \begin{bmatrix} F_{xrl} \\ F_{xrr} \end{bmatrix}$$

The Figure 4 illustrates the closed loop system. Considering the control law $Bu = [0, k\dot{\psi}]^T$, where $k > 0$ is a controller gain, the system is reduced to:

$$\dot{x} = A_r x + C\delta \tag{31}$$

where

$$A_r = \begin{bmatrix} -\frac{C_{\alpha f}+C_{\alpha r}}{m_{CoG}v_{CoG}} & \frac{C_{\alpha r}l_r + C_{\alpha f}l_f}{m_{CoG}v_{CoG}^2} - 1 \\ \frac{C_{\alpha r}l_r - C_{\alpha f}l_f}{J} & -\frac{C_{\alpha r}l_r^2 + C_{\alpha f}l_f^2}{Jv_{CoG}} + k \end{bmatrix},$$

$$C = \begin{bmatrix} \frac{C_{\alpha f}}{m_{CoG}v_{CoG}} \\ \frac{C_f l_f}{J} \end{bmatrix}$$

Considering δ as a small perturbation such that $\delta \approx 0$ and performing a Laplace stability analysis for $\dot{\psi}$ in order to find the values of k that gives a stable system, it is found that:

$$k < \left[-\frac{C_{\alpha f} + C_{\alpha f}}{m_{CoG}v_{CoG}}\right] + \left[-\frac{C_{\alpha r}l_r^2 + C_{\alpha f}l_f^2}{Jv_{CoG}}\right] \tag{32}$$

TABLE I
PARAMETERS USED FOR THE THREE-WHEELED VEHICLE MODEL SIMULATION.

Parameters:	Value	Units
b_l	0.525	m
b_r	0.525	m
$C_{\alpha f}$	$120,000$	N/rad
$C_{\alpha r}$	$155,000$	N/rad
g	9.8	m/s^2
h	0.54	m
J	$1,111$	kgm^2
l_f	1.103	m
l_r	0.922	m
m	747	kg
v_{CoG}	13.9	m/s

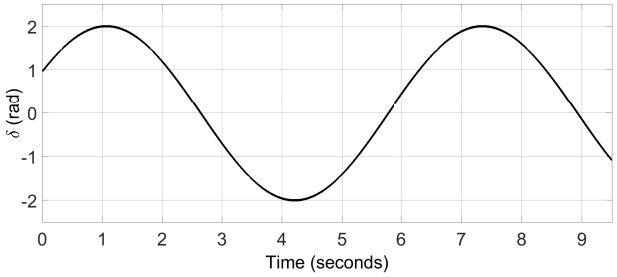

Fig. 5. Front steering maneuver.

V. SIMULATIONS

In order to evaluate the performance of the proposed controller to mitigate the Rollover Index, Simulink and CarSim simulations are performed using a three-wheeled vehicle which model parameters are shown in Table I. In Figure 5 is shown the front steering behaviour that represents a double lane change and is selected for lifting a rear wheel. Due to the fact that the proposed mathematical model does not take into account a suspension system and the CarSim model does, the spring rate was set as very high in CarSim to simulate a non-suspension Delta tricycle. Considering the tricycle parameters of Table I it is obtained that $k < -44.47$ in order that the system to be stable. Hydraulic actuators are used for simplicity (electric ir pneumatic ones can be used instead depending on application): CarSim provides braking pressures as variable inputs for the rear wheels (P_{br}, P_{bl}). The actuators models are chosen as linear ($F_{xrj} = 380P_{bj}$, where j is left/right). Choosing values of k it is found that if the magnitude of the gain is selected high, this lead to higher values of breaking pressure and thus an aggressive braking such that the tire slips (the CarSim vehicle hasn't be programmed with an ABS). On the other hand, if the magnitude of the gain is lower, the breaking pressure does not seem to provide a proper rollover mitigation. The gain is then selected as $k = -80$ which is consistent with the stability condition (32). In Figure 7 is shown the braking pressure in the left and right rear wheels; it is easy to see that the braking pressure follows the rollover risk estimation. In Figure 6 is shown a comparative for the RI and the vertical forces (which were normalized by dividing them by $m*g$) in open loop (upper plot) vs closed loop (lower plot); it is easy to see that the controller mitigates the rollover.

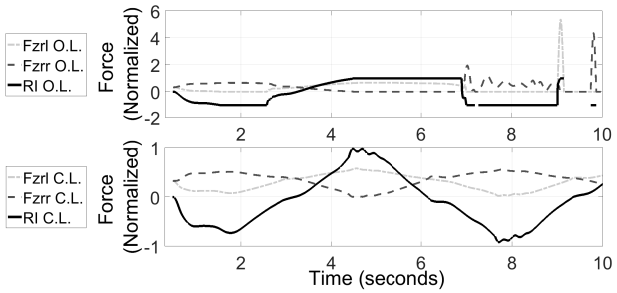

Fig. 6. RI and vertical forces comparison in open loop (upper plot) and closed loop (lower plot).

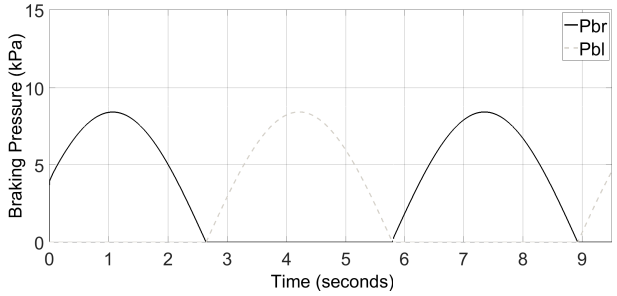

Fig. 7. Braking pressure in the left and right wheels at the rollover mitigation.

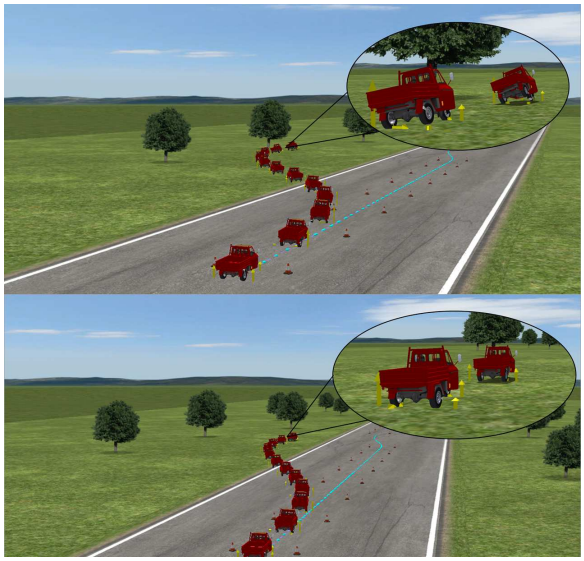

Fig. 8. Illustrative comparative of the dynamic behaviour of the vehicle in open loop (upper capture) and closed loop using the rear differential braking (lower capture).

Finally, in Figure 8 is shown a pictoric comparative of the dynamic behaviour of the vehicle for open loop vs closed loop; it is very illustrative the use of this kind of animations to have a real expectative of the dynamics of the vehicle. Figure 8 shows that the rollover is effectively mitigated while in closed loop conditions. This is, the controller enhances the safety during curves including the case of a noncentered CoG (simulations of CoG changes are left for a future work).

VI. Conclusions

In this paper, a new estimation of the rollover risk in delta tricycles is developed as a rollover index in allusion to such estimation in vehicles with 4 or more wheels. It is worth to mention that at present, the authors can't locate a similar approach for the estimation of the rollover risk in dynamic conditions. A dynamic model of the tricycle that is intended to estimate the rollover index is obtained and validated with a non-linear model, showing a very close behaviour of the model: The proposed rollover index is able to predict and detect a rollover. The rollover index include the contribution to the risk due to the lateral and longitudinal location of the CoG. Also, a controller based on rear differential braking for the rollover risk mitigation in tricycles is presented. The differential braking strategy effectively can reduce or mitigate the rollover as shown by simulations. It is the intention of this work, to motivate the increase of safety research in three-wheeled vehicles .

Acknowledgment

Edgar A. Vázquez Rodríguez acknowledges financial support from Consejo Nacional de Ciencia y Tecnología, México CVU856319.

References

[1] S. E. Harding, M. G. Badami, C. C. Reynolds, and M. Kandlikar, "Auto-rickshaws in indian cities: Public perceptions and operational realities," *Transport policy*, vol. 52, pp. 143–152, 2016.

[2] P. P. Akshay Mani, "Review of literature in india's urban auto-rickshaw sector: A synthesis of findings," October 2012. [Online]. Available: https://wrirosscities.org/research/publication/review-literature-indias-urban-auto-rickshaw-sector-synthesis-findings

[3] T. Economist. (2014, February) Three-wheeled transport. tuk-tuking the wolrd by storm. [Online]. Available: https://www.economist.com/business/2014/02/22/tuk-tuking-the-world-by-storm

[4] G. Wu, A. Inderbitzin, and C. Bening, "Total cost of ownership of electric vehicles compared to conventional vehicles: A probabilistic analysis and projection across market segments," *Energy Policy*, vol. 80, pp. 196–214, 2015.

[5] T. R. Hawkins, B. Singh, G. Majeau-Bettez, and A. H. Strømman, "Comparative environmental life cycle assessment of conventional and electric vehicles," *Journal of Industrial Ecology*, vol. 17, no. 1, pp. 53–64, 2013.

[6] I. Neumann, P. Cocron, T. Franke, and J. F. Krems, "Electric vehicles as a solution for green driving in the future? a field study examining the user acceptance of electric vehicles," in *Proceedings of the European Conference on Human Interface Design for Intelligent Transport Systems, Berlin, Germany*, 2010, pp. 445–453.

[7] N. DeForest, J. Funk, A. Lorimer, B. Ur, I. Sidhu, P. Kaminsky, and B. Tenderich, "Impact of widespread electric vehicle adoption on the electrical utility business-threats and opportunities," *Center for Entrepreneurship and Technology (CET) Technical Brief*, no. 2009.5, 2009.

[8] N. H. T. S. Administration *et al.*, *Traffic Safety Facts, 2001. Overview*. National Center for Statistics and Analysis, 2001.

[9] ——, "Dot announces proposal to add rollover ratings to auto safety consumer information program," *NHTSA Now*, vol. 6, no. 7, 2000.

[10] P. Giovanni, M. Barić, L. Glielmo, E. H. Tseng, and B. Francesco, "Robust vehicle lateral stabilization via set-based methods for uncertain piecewise affine systems: Experimental results," in *2011 50th IEEE Conference on Decision and Control and European Control Conference, CDC-ECC 2011*, 2011.

[11] C. Bardawil, R. Talj, C. Francis, A. Charara, and M. Doumiati, "Integrated vehicle lateral stability control with different coordination strategies between active steering and differential braking," in *Intelligent Transportation Systems (ITSC), 2014 IEEE 17th International Conference on*. IEEE, 2014, pp. 314–319.

[12] S. Zhang, T. Zhang, and S. Zhou, "Vehicle stability control strategy based on active torque distribution and differential braking," in *Measuring Technology and Mechatronics Automation, 2009. ICMTMA'09. International Conference on*, vol. 1. IEEE, 2009, pp. 922–925.

[13] J. Lee and K. Yi, "Development of a combined steering torque overlay and differential braking strategy for unintended lane departure avoidance," in *Intelligent Transportation Systems (ITSC), 2011 14th International IEEE Conference on*. IEEE, 2011, pp. 1223–1230.

[14] M. R. Licea and I. Cervantes, "Robust indirect-defined envelope control for rollover and lateral skid prevention," *Control Engineering Practice*, vol. 61, pp. 149–162, 2017.

[15] Z. Peng and G. Ning, "2 dof lateral dynamic model with force input of skid steering wheeled vehicle," in *Transportation Electrification Asia-Pacific (ITEC Asia-Pacific), 2014 IEEE Conference and Expo*. IEEE, 2014, pp. 1–5.

[16] K. Stefan, B. De Mersseman, H. Knight-Newbury, and J. A. Marcari, "System and method for preventing rollover," Aug. 28 2007, uS Patent 7,261,303.

[17] A. Amodio, M. Corno, G. Panzani, and S. Savaresi, "Differential braking-based anti-rollover control for non-tilting narrow-track vehicles," in *Control Technology and Applications (CCTA), 2017 IEEE Conference on*. IEEE, 2017, pp. 1880–1885.

[18] R. Kamnik, F. Boettiger, and K. Hunt, "Roll dynamics and lateral load transfer estimation in articulated heavy freight vehicles," *Proceedings of the Institution of Mechanical Engineers, Part D: Journal of Automobile Engineering*, vol. 217, no. 11, pp. 985–997, 2003.

[19] J. H. Woodrooffe, *Review of Canadian experience with the regulation of large commercial motor vehicles*. Transportation Research Board, 2010, vol. 671.

[20] N. Moshchuk and S.-K. Chen, "Vehicle rollover detection index," in *ASME 2009 International Mechanical Engineering Congress and Exposition*. American Society of Mechanical Engineers, 2009, pp. 583–587.

[21] S. Solmaz, M. Corless, and R. Shorten, "A methodology for the design of robust rollover prevention controllers for automotive vehicles with active steering," *International Journal of Control*, vol. 80, no. 11, pp. 1763–1779, 2007.

[22] V. Tsourapas, D. Piyabongkarn, A. C. Williams, and R. Rajamani, "New method of identifying real-time predictive lateral load transfer ratio for rollover prevention systems," in *American Control Conference, 2009. ACC'09.* IEEE, 2009, pp. 439–444.

[23] G. A. D. Thomas Lich, ZWEEGE Remco TEN, "An active rollover prevention device for a three-wheeled vehicle," Nov. 17 2017, international Publacation Number WO2016180637A1.

[24] D. Mercier, Y. Berthiaume, R. Biron, and A. Massicotte, "Roll-related reactive system," Dec. 5 2006, uS Patent 7,143,853.

[25] A. Zandieh, "Dynamics of a threewheel vehicle with tadpole design," Master's thesis, University of Waterloo, 2015.

[26] V. M. Karanam and A. Ghosal, "Studies on the wobble mode stability of a three-wheeled vehicle," *Proceedings of the Institution of Mechanical Engineers, Part D: Journal of Automobile Engineering*, vol. 227, no. 8, pp. 1200–1209, 2013.

[27] M. R. Babu, "Lateral dynamics of bajaj rear engine auto-rickshaw," Master's thesis, University of Roorkee, 1995.

[28] T. Gawade, S. Mukherjee, and D. Mohan, "Six-degree-of-freedom three-wheeled-vehicle model validation," *Proceedings of the Institution of Mechanical Engineers, Part D: Journal of Automobile Engineering*, vol. 219, no. 4, pp. 487–498, 2005.

[29] T. D. Gillespie, "Fundamentals of vehicle dynamics. warrendale, pa: Society of automotive engineers," 1992.

[30] U. Kiencke and L. Nielsen, "Automotive control systems: for engine, driveline, and vehicle," 2000.

[31] M. A. Rodríguez Licea, "Estrategias de control conmutado robusto para mitigar volcadura y derrape en vehículos con ruedas," Ph.D. dissertation, Instituto Potosino de Investigación Científica y Tecnológica, 2015.

[32] J. Pearson, "Vehicle weights and dimension limits within the nafta partnership," *Task Force on VW&D Policy*, vol. 27, 2002.